



The urban greenness score: A satellite-based metric for multi-decadal characterization of urban land dynamics



Agatha Czekajlo^{a,*}, Nicholas C. Coops^a, Michael A. Wulder^b, Txomin Hermosilla^b, Yuhao Lu^c, Joanne C. White^b, Matilda van den Bosch^{d,e}

^a The Department of Forest Resources Management, University of British Columbia, 2424 Main Mall, Vancouver, BC V6T 1Z4, Canada

^b Canadian Forest Service, Pacific Forestry Centre, Natural Resources Canada, 506 West Burnside Road, Victoria, BC, V8Z 1M5, Canada

^c School of Architecture and Landscape Architecture, University of British Columbia, 2260 West Mall, Vancouver, BC, V6T 1Z4, Canada

^d School of Population and Public Health, The University of British Columbia, 2206 East Mall, Vancouver, BC, V6T 1Z3, Canada

^e The Department of Forest and Conservation Sciences, The University of British Columbia, 2424 Main Mall, Vancouver, BC, V6T 1Z4, Canada

ARTICLE INFO

Keywords:
Urban
Vegetation
Time series
Landsat
Spectral unmixing
Canada

ABSTRACT

Canada's urban areas have experienced extensive growth over the past quarter century; however, there has been no consistent, spatially explicit approach for quantifying the loss and gain of greenness in cities nationally. Herein, we developed a novel urban greenness score metric using greenness fractions from a multi-decadal time series (1984–2016) of spectrally unmixed annual Landsat satellite image composites to characterize final year (2016) greenness and its overall change for 18 major Canadian urban areas, summarized by census dissemination area (DA). The applied validation procedure confirmed correlation coefficients (ρ) ranging from 0.67 – 0.85 between reference and estimated greenness fractions, indicating that spectral unmixing is an appropriate method for extracting urban greenness from a time series of medium spatial resolution satellite imagery. Most DAs across Canada sustained a moderate (~ 20 % – 40 %) or low ($\leq 20 \%$) level of greenness between 1984 and 2016, but overall there was a decreasing trend in greenness. Eastern urban areas maintained the most greenness over time, while urban areas in the Prairies had the greatest increase in greenness. Densely populated urban areas experienced the greatest loss in greenness (16 % of DAs); whereas, urban areas with a moderately-low density experienced the greatest increase (14 % of DAs). In agreement with previous studies, we found that greenness was negatively associated with urban infilling, with lower greenness levels typically found in urban cores, and greenness loss most often found in the urban periphery in conjunction with urban expansion. Methods presented in this analysis take advantage of the open and longstanding Landsat archive, as well as multiple spatial scales, including sub-pixel unmixing techniques, pixel level greenness fraction data summarized for management units, and analysis conducted nationally. The developed urban greenness score provides a comprehensive framework to understand current urban greenness and relate it to its recent past, which supports long-term strategic planning, and can be transferred to other regions across spatial and temporal scales.

1. Introduction

Globally, urban areas have been consistently growing since the turn of the 20th century with urban populations growing at twice the rate of the overall global population increase (Angel et al., 2011; Seto et al., 2011; United Nations, 2018). Canada has experienced a steady increase in urban populations since the late 1800s, with the percent of urban residents growing from 15 % to 80 % over the past 150 years (Statistics Canada, 2018). During a shorter time period, from 1971 to 2011, the

built-up area in Canada increased by 157 %, from 5,651 km² to 14,546 km² (Statistics Canada, 2016) and national projections indicate continued population growth (Statistics Canada, 2017a). Large Census Metropolitan Areas, including Calgary, Toronto, and Vancouver, in particular increased their built-up area (ranging from 102 to 220 %) as their population density increased (12 – 14 %; Statistics Canada, 2016). However, the rate of urbanization varies regionally due to a multitude of factors, including natural landscape features and barriers, population growth, accessibility, land value, and municipal and/or regional

* Corresponding author

E-mail addresses: a.czekajlo@alumni.ubc.ca (A. Czekajlo), nicholas.coops@ubc.ca (N.C. Coops), mike.wulder@canada.ca (M.A. Wulder), txomin.hermosillagomez@canada.ca (T. Hermosilla), luyhao@mail.ubc.ca (Y. Lu), joanne.white@canada.ca (J.C. White), matilda.vandenbosch@ubc.ca (M. van den Bosch).

policies (Brueckner and Fansler, 1983; Glaeser and Kahn, 2003; Kulish et al., 2012; Saiz, 2010).

While cities are centers of prosperity, education, and culture, they typically also have high levels of air pollution, noise, and crowding, all with negative effects on human health (Block et al., 2018; Krefis et al., 2018; Muzet, 2007). One way for urban planners to mitigate the negative impacts of urbanization and create more sustainable and healthy cities is by incorporating more green spaces (Un-Habitat, 2016). Green spaces include public or private vegetated areas, such as parks, street trees, natural areas like wetlands or grasslands, and residential gardens (Kumagai, 2011; Haaland and Konijnendijk van den Bosch, 2015). They provide a range of regulating ecosystem services to urban areas, such as heat reduction, flood mitigation, and air purification (Livesley et al., 2016), as well as direct public health benefits like improving the physical, mental, and social wellbeing of individuals (Hartig et al., 2014; van den Bosch and Ode Sang, 2017; van den Bosch and Bird, 2018). However, despite the benefits of green spaces for environmentally sustainable cities, they are typically not evenly distributed within urban areas (Heynen et al., 2006; Landry and Chakraborty, 2009; Tooke et al., 2010) and are threatened by continued urban growth (Fragkias et al., 2013).

Planning for and managing urban green spaces is key to ensuring their functionality and potential for providing ecosystem services, as well as the general sustainability of cities. Remote sensing technologies have the potential to support the information needs of planners and civic managers by providing frequent, accurate, and cost-effective spatial information at an appropriate scale and expedited rate (Patino and Duque, 2013). Across a variety of spatial resolutions, spectral unmixing methods have been used extensively in remote sensing research to derive spectrally differentiated characteristics of a surface. During a spectral unmixing procedure, spectral characteristics of determined pure pixels in an image are extracted and compared across remaining pixels to determine the fractional component of each characteristic (Small, 2001). Using spectral unmixing, various forms of vegetation have been distinguished from other surfaces, such as bare soil (Asner and Heidebrecht, 2002), impervious surface (Lu and Weng, 2006), or snow (Vikhamar and Solberg, 2003). The method has also been used to quantify the fraction of vegetation across international urban environments by differentiating between high albedo, dark, and green vegetated surfaces (Lu et al., 2017). Using a multitude of spectral unmixing variations, the proportion of urban vegetation greenness can be quantified at the pixel level for extracting area-based green space information. Unlike the Normalized Difference Vegetation Index (NDVI), which has been extensively used to measure vegetation in many contexts, including urban green spaces and at various spatial scales (e.g. Atasoy, 2018; Fung and Siu, 2001; Hidayat and Ridwan, 2018; Li et al., 2015), spectral unmixing avoids errors caused by interactions between detected spectral signatures (Liu and Kafatos, 2007). Additionally, sensor-specific band characteristics and unexplained atmospheric interactions may contribute to the overall uncertainty of NDVI (van Leeuwen et al., 2006). This may pose problems for the analysis of large spatial extents, such as vegetation greenness across Canadian cities. Spectral unmixing has been demonstrated to produce accurate and reliable information regarding urban vegetation greenness and its changes over time, with informative examples over limited extents of time and space (Haase et al., 2019; Lu et al., 2017; Okujeni et al., 2013; Phinn et al., 2002; Powell and Roberts, 2010, 2008; Small, 2001; Tooke et al., 2009), offering insights towards investigations over longer time periods and areal extents.

Given the trajectory of urbanization globally, effective spatial monitoring of urban growth and green space dynamics is critical to achieve sustainable urban development. Medium spatial resolution (10–100 m sided pixels) remote sensing platforms, such as the series of Landsat satellites, provide freely-available and long-term data appropriate for studying urban dynamics around the world. Landsat satellite imagery, in particular, is suitable to utilize for urban landscape analyses

as it has been systematically acquired over several decades (Schneider et al., 2009; White et al., 2014; Woodcock et al., 2008; Wulder and Coops, 2014). Given that urban planning and management is conducted on a range of spatial scales, information attained from medium-resolution satellite imagery can be appropriately applied for a variety of needs. Additionally, recent advancements in data acquisition and processing methods have facilitated the creation of accurate, medium spatial resolution time series products at annual intervals from large datasets (Schneider, 2012; White et al., 2014; Zhu et al., 2019). With advanced computing abilities and access to reliable, long-term satellite imagery, it is now possible to develop a standardized approach to map past and current urban vegetation greenness in a reproducible fashion.

The overall goal of this study is to develop a novel urban greenness score that incorporates the current state of urban greenness with historic trends. We aim to characterize and temporally assess Canadian urban greenness using the score, which integrates the final year and overall change of unmixed greenness fractions derived from annual gap-free Landsat surface reflectance products. To address these aims we: (i) apply spectral unmixing for extracting the pixel level greenness fraction; (ii) assess the accuracy of extracted greenness fractions; (iii) develop an urban greenness score that combines status and trends in greenness fractions over time, and; (iv) apply the urban greenness score to major urban areas in Canada and demonstrate the utility of the urban greenness score for national level urban monitoring. Our developed approach offers a number of new insights and innovations. First, we believe this study to be one of the pioneering examples of both applying spectral unmixing across extremely large spatial scales, as well as exploiting the long term archival data made available by the Landsat program to extract endmembers' fractions annually for multi-decadal time series. Second, while urban studies using Landsat imagery are not uncommon, the condensing of this high dimensional spectral data in a simple and interpretable greenness score can then be applied across a range of urban environments in Canada and inform future applications globally.

2. Data and methods

We developed an urban greenness score that summarizes greenness across 18 Canadian urban areas, located across four geographic strata and across a population density gradient (high, moderately-high, moderately-low, and low). The open and long-standing Landsat data archive was used to map urban greenness consistently over the 33-year period (1984–2016). A linear spectral unmixing algorithm was applied to each multi-temporal, geographic, strata-based, image stack to extract the greenness fraction of each urban area's pixels for all 33 years. The greenness fraction was smoothed temporally across the study time period using locally weighted scatterplot smoothing (LOESS) at the pixel level for each urban area. The urban greenness score was developed by combining information on the final year (2016) greenness fraction and the 33-year change in greenness. The urban greenness score was summarized on the census dissemination area (DA) level and analysis was conducted within the urban area, as well as between urban areas by strata and population density groups. Fig. 1 shows a workflow of the methods. Software used for image and data processing includes IDL 8.7, ENVI 5.5, ArcMap 10.6, FETEX 2.0 (Ruiz et al., 2011), and R (ver. 3.5.2; R Core Team, 2018) for statistical analysis. Using R, clustering was implemented using the *fastcluster* package (Müllner, 2013), and the Mann-Kendall and TS estimators were computed using the *wq* package (Jassby and Cloern, 2017).

2.1. Study area

We analyzed 18 urban areas in Canada (Fig. 2) that were either provincial capitals or had a population greater than 100,000 persons in 2016, representing about 60 % of Canada's population at the time (Statistics Canada, 2017b). In total over 40,000 km² were considered as

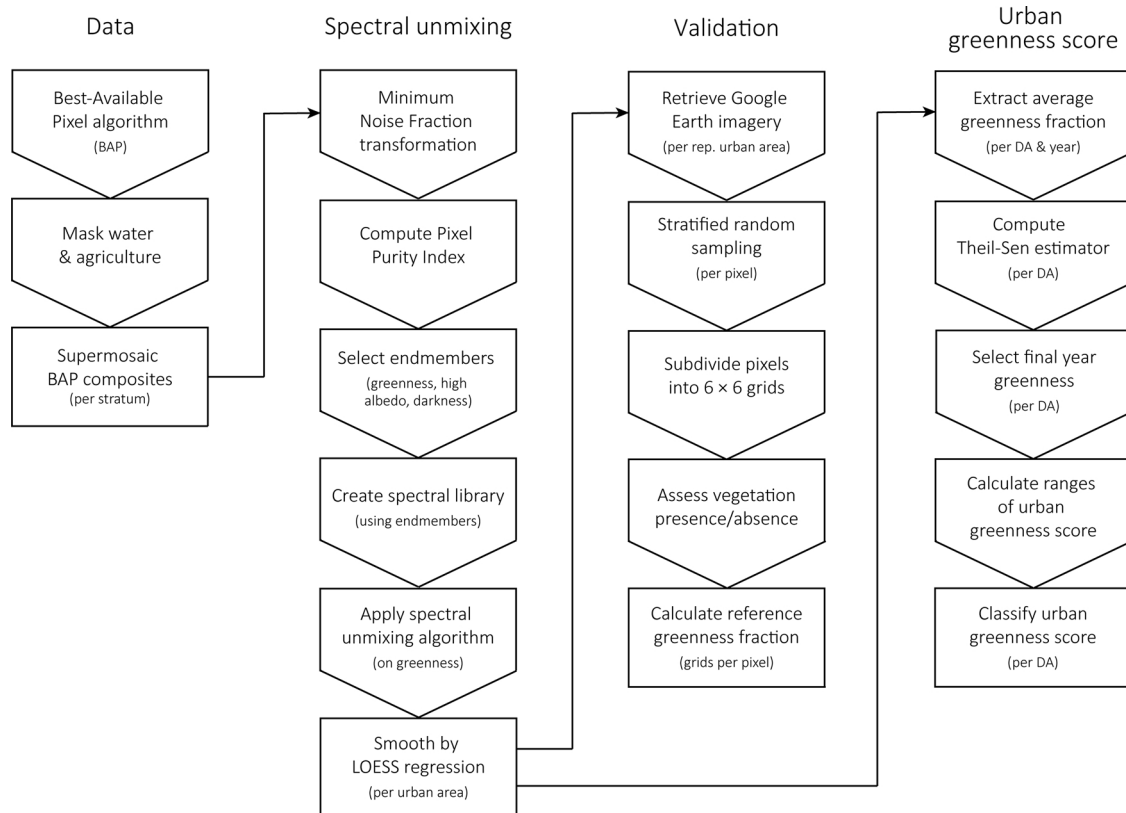


Fig. 1. Workflow diagram of methods used to derive the urban greenness score, specifying data used, as well as the steps related to spectral unmixing, validation, and the development of the urban greenness score.

urban area in this analysis. An urban area in this study is defined as the dissemination areas (DAs) within the urban core (i.e. census metropolitan area or census agglomeration), as well as all directly

adjoining DAs. The spatial unit of DAs was chosen as it is the smallest for which Canadian census data are disseminated and they are relatively stable through time. A DA contains between 400 and 700 people

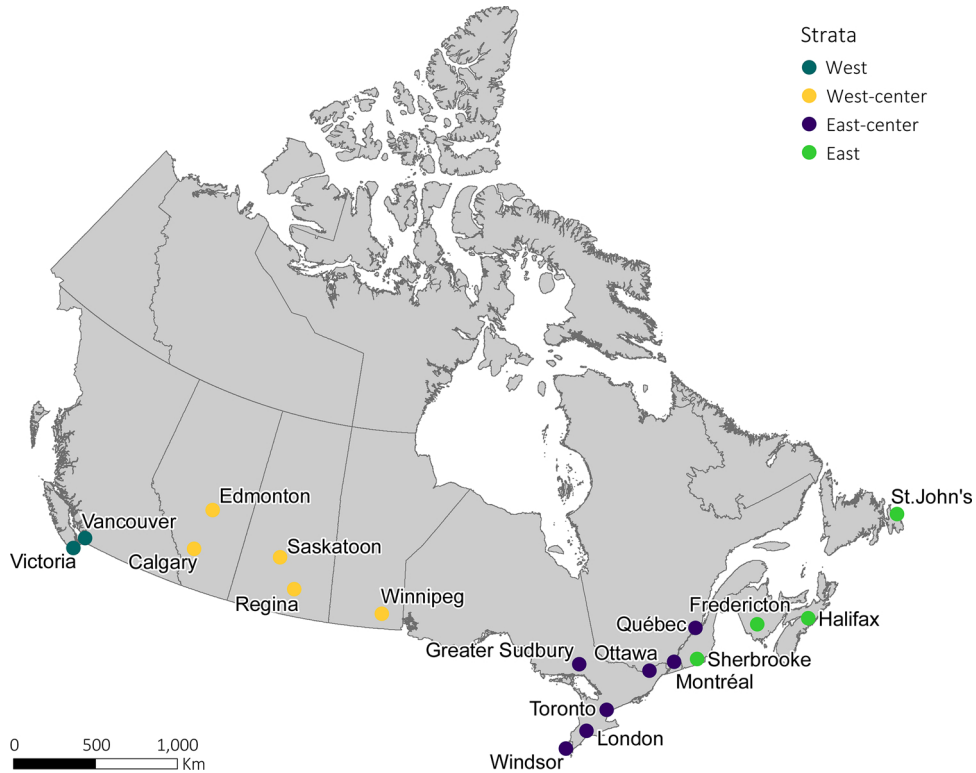


Fig. 2. Locations of the 18 selected Canadian urban areas used in this study, by strata.

Table 1

Summary of population density groups (High, Moderately-high (Mod-high), Moderately-low (Mod-low), and Low), including the number of 2016 dissemination areas (DAs) used in this analysis, as well as their total geometric area (km^2), and average 2016 DA level population density (persons per land area (km^2)).

Population density group	DA count	Area (km^2)	Population density (persons per km^2)
High	20,578	10,746	6,148
Mod-high	5,689	9,541	4,044
Mod-low	3,296	2,079	3,360
Low	2,464	20,454	2,248

(Statistics Canada, 2011). DAs with more than 50 % of pixels encompassed by agriculture or water masks were excluded from this analysis and did not contribute to the total geometric area of an urban area, stratum, or population density group.

Urban areas were grouped into four geographic strata that share similar vegetation types (west, west-center, east-center, and east; Marshall et al., 1999), and subsequently distinguished in the spectral unmixing procedure. Population density is a key component in Canada's current urban classification system used to delineate population centers from rural areas (Statistics Canada, 2011) as Canadian cities typically follow the pattern of decreasing population densities with distance from the urban core (Turcotte, 2008). As a result, urban areas were stratified by average population density using Ward's method of hierarchical clustering (Ward, 1963). Using four groups derived from the clustering procedure, urban areas were assigned a population density-based group corresponding to their relative level of population density: High, Moderately-high (Mod-high), and Moderately-low (Mod-low), and Low. Table 1 provides a summary of each population density group's DA count (2016), as well as its total geometric area and average 2016 DA level population density. A similar summary for each urban area is provided in Table 2, including each the respective stratum and population density group.

2.2. Data

Landsat imagery with less than 70 % cloud cover, acquired during the summer growing period (August 1st \pm 30 days) from 1984 to 2016, were selected for the basis of the analysis. For each year of

analysis, the best-available pixel algorithm (BAP; White et al., 2014) was employed to choose the highest quality pixel from selected Landsat imagery and create a single annual cloudless composite of each urban area. All 33 annual Landsat BAP composites for each urban area of a given stratum were analyzed simultaneously in the spectral unmixing procedure. Yearly land cover maps derived from the Virtual Land Cover Engine (VLCE; Hermosilla et al., 2018) were used to identify and exclude agricultural and water pixels.

2.3. Spectral unmixing procedure

The methods for spectral unmixing built upon those of Lu et al. (2017), and in part Small and Lu (2006) and Tooke et al. (2009). The unmixing analysis was conducted for urban areas of the same stratum to ensure greenness levels were representative of vegetation inherent to each geographic region. First, a minimal noise fraction transformation (MNF; Green et al., 1988) was performed on each stratum to extract three MNF components that explained over 98 % of variance. Next, the pixel purity index (PPI) was computed and used to identify image-based endmembers that best describe the mixing volume (Bateson and Curtiss, 1996; Boardman, 1993; Boardman et al., 1995). Using the PPI, three endmembers (i.e. spectrally pure pixels) of greenness (i.e. green vegetation), high albedo (i.e. reflected brightness) and darkness were selected for each stratum. Endmembers were differentiated spectrally by their relative distributions across the first, second and third MNF components. Pixels characterized by the greenness endmember include highly manicured grass, such as those in golf courses, as well as treed areas like parks or natural forests. The high albedo endmember pixels ranged from impervious urban surfaces to rocky surfaces in natural areas. Dark endmember pixels include shadows, such as those cast by high rise buildings or dense multi-level forests.

From this three-endmember model, a spectral library was built for each geographic stratum and then a sub-pixel linear spectral unmixing algorithm was applied to extract the fractions of greenness, high albedo, and darkness for each individual urban area. This was done using the following equation:

$$R = \sum_{i=1}^n f_i e_i + \varepsilon$$

where R is the unmixed surface reflectance; f_i is the endmember image fraction; e_i is the endmember's surface reflectance value; n is the

Table 2

Summary of urban areas, including their respective stratum and province, number of 2016 dissemination areas (DAs) used in analysis, as well as their total geometric area (km^2), total 2016 population (persons), average 2016 DA level population density (persons per land area (km^2)), and assigned population density group (High, Moderately-high (Mod-high), Moderately-low (mod-low), and Low).

Stratum	Province	Urban area	DA count	Area (km^2)	Total population (persons)	Population density (persons per km^2)	Population density group
West	British Columbia	Victoria	541	633	349,598	3,226	Mod-low
		Vancouver	3,663	3,335	2,536,528	6,011	High
West-center	Alberta	Edmonton	1,441	1,033	987,371	3,554	Mod-low
		Calgary	1,589	775	1,116,102	4,088	Mod-high
	Saskatchewan	Saskatoon	343	99	214,409	3,302	Mod-low
		Regina	385	138	209,250	2,951	Mod-low
	Manitoba	Winnipeg	1,095	659	652,264	4,158	Mod-high
East-center	Ontario	Greater Sudbury	255	4,289	155,223	1,462	Low
		Windsor	745	321	409,604	2,713	Low
		London	603	176	382,512	3,313	Mod-low
		Toronto	10,881	5,488	7,653,628	5,704	High
		Ottawa	1,847	6,007	1,189,369	4,008	Mod-high
	Québec	Montréal	6,162	1,923	3,782,524	7,013	High
		Québec City	1,164	2,100	704,327	3,934	Mod-high
East	Québec	Sherbrooke	273	930	178,040	2,310	Low
	New Brunswick	Fredericton	164	3,483	101,733	961	Low
	Nova Scotia	Halifax	741	10,700	471,062	2,365	Low
	Newfoundland and Labrador	St. John's	306	732	190,778	2,123	Low

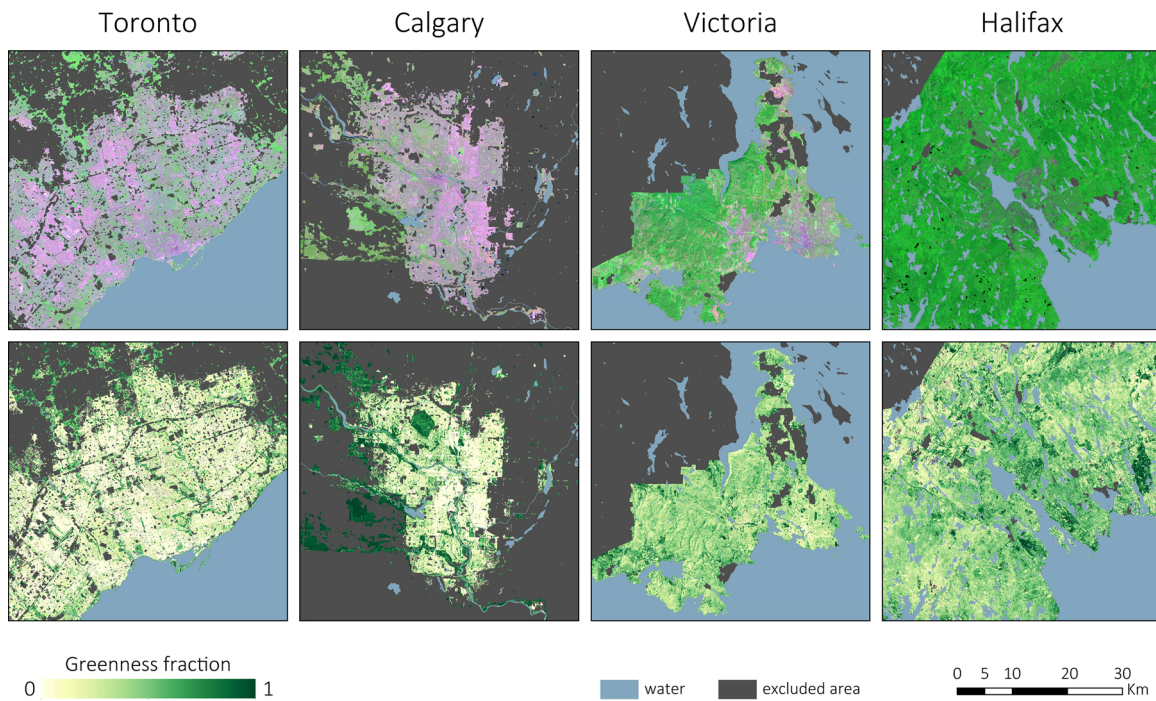


Fig. 3. 2016 Landsat BAP composites (top panels; RGB: SWIR2, NIR, G) and smoothed unmixed greenness fraction results (bottom panels) of parts of Toronto (high population density; east-center stratum), Calgary (mod-high population density; west-center stratum), Victoria (mod-low population density; west stratum), and Halifax (low population density; east stratum). A colour version of this figure is available in the online version of this article.

number of endmembers, and; ϵ is the root mean square error. The extracted greenness fraction images were subset and temporally smoothed using locally weighted regression method (LOESS; Cleveland and Devlin, 1988) to minimize intra-seasonal fluctuations of urban vegetation. Fig. 3 shows the comparison between the Landsat BAP composites and the resulting greenness fraction for four example urban areas (Toronto, Calgary, Victoria, and Halifax), each representing a different stratum and population density group. The greenness fraction generally follows the pattern of impervious/vegetated surfaces.

2.4. Validation of greenness fraction

We validated the determination of greenness fractions for corresponding years throughout the 33-year time series using high spatial resolution images provided by Google Earth. Validation images were chosen based on two criteria: (i) being cloud-free, and (ii) collected during the Canadian growing season. Since cloud-free Google Earth images during the growing season vary in quality and availability, we chose one representative urban area per stratum: Vancouver (west), Edmonton (west-center), Toronto (east-center), and Fredericton (east). Three validation images from varying years were chosen for each of the four urban areas: Vancouver (2003, 2008, and 2015), Toronto (2002, 2009, and 2015), Edmonton (2010, 2012, and 2015) and Fredericton (2005, 2010, and 2011). For each of the twelve images (i.e. three images per year per urban area), up to 100 pixels per image were selected using stratified random sampling (with 10 % greenness fraction classes) within each urban area boundary, and then subdivided into 6×6 m grids (i.e. 25 grids per pixel). An interpreter, blind to the greenness fraction of each pixel, assessed the presence/absence of green vegetation for each grid. The reference greenness fractions were calculated using the proportion of presence to absence values of all 25 grids per pixel. Poor quality pixels of imagery shared in Google Earth were excluded from the validation results after closer inspection. Spearman's correlation coefficients (ρ) were employed to compare the non-parametric estimated (i.e. unmixed) and reference greenness fractions of all pixels of a given year of each representative urban area.

2.5. Urban greenness score

On the DA level, average greenness (referred to simply as 'greenness') was calculated as a percentage from the time series of annual, smoothed, unmixed greenness fractions (ranging between 0–1). The urban greenness score, which categorizes the change in greenness during the time series in relation to the final greenness level of a given year, is shown as Fig. 4. For this study, the final greenness indicated the value from the year 2016, and change in greenness was calculated using

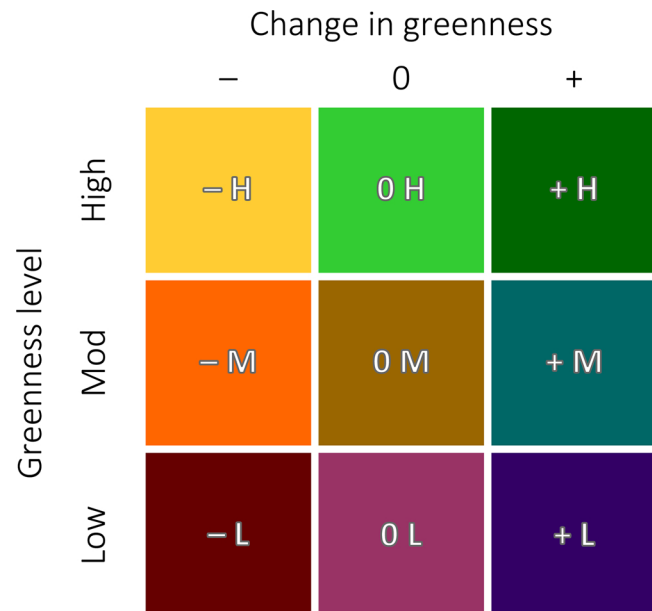


Fig. 4. Urban greenness score matrix showing final greenness (rows = low (L), moderate (M), and high (H)) in relation to the change in greenness (columns = decrease (-), zero (O), and increase (+)). A colour version of this figure is available in the online version of this article.

the Theil-Sen estimator (i.e. TS; Sen, 1968; Theil, 1992) of all 33 years of the time series. Change in greenness was categorized into three levels (decrease (-), zero (0), and increase (+)) using a positive and negative unit of standard deviation for all DAs. The final greenness of all DAs was categorized into three levels (low (*L*), moderate (*M*), and high (*H*)) using natural breaks (Jenks), which identifies class breaks by minimizing within-group variation and maximizing between-group variation (Coulson, 1987; Jenks and Caspall, 1971). The natural breaks classification was chosen in part for its common usage, data-driven determination of breaks, as well as its successful use in a similar circumstance of classifying a remotely sensed vegetation index by Anchang et al. (2016). As the urban greenness score is meant to provide a practical yet reliable method to identify areas with relatively higher or lower greenness, which may subsequently be assessed at a finer scale for management purposes, the natural breaks classification harnesses the inherent distribution of greenness across all DAs and avoids subjective class distinctions.

3. Results

3.1. Validation of unmixed greenness fraction

The estimated greenness fractions largely correlated with the

reference values (Fig. 5), with Spearman's correlation coefficients (ρ) between estimated (i.e. unmixed) and reference greenness fractions of 0.85, 0.67, 0.71, and 0.80 for the urban areas of Vancouver, Edmonton, Toronto, and Fredericton, respectively. Although outliers were present for all, urban areas, Edmonton exhibited the most outliers and had the lowest rank correlation ($\rho = 0.67$). Edmonton also showed higher estimated median values compared to its reference values than Vancouver even though both share similar estimated and reference median greenness fractions (Edmonton = 0.54 and 0.50, and; Vancouver = 0.53 and 0.52, respectively). Toronto and Fredericton both showed lower estimated median greenness fractions (0.50 and 0.52, respectively) in comparison to their reference values (0.56 for both).

3.2. Evolution of greenness fraction through time

A crucial component of the novel urban greenness score is the change in greenness extracted from the entire time series of greenness fraction data. Fig. 6 shows a portion of Toronto DAs classified by their change in greenness over the 33-year period, the final (2016) level of greenness, as well as the time series of select DAs' greenness fractions that achieve different urban greenness scores. The integration of greenness change provides a temporal context to the single-year greenness level that differentiates areas of different urban greening

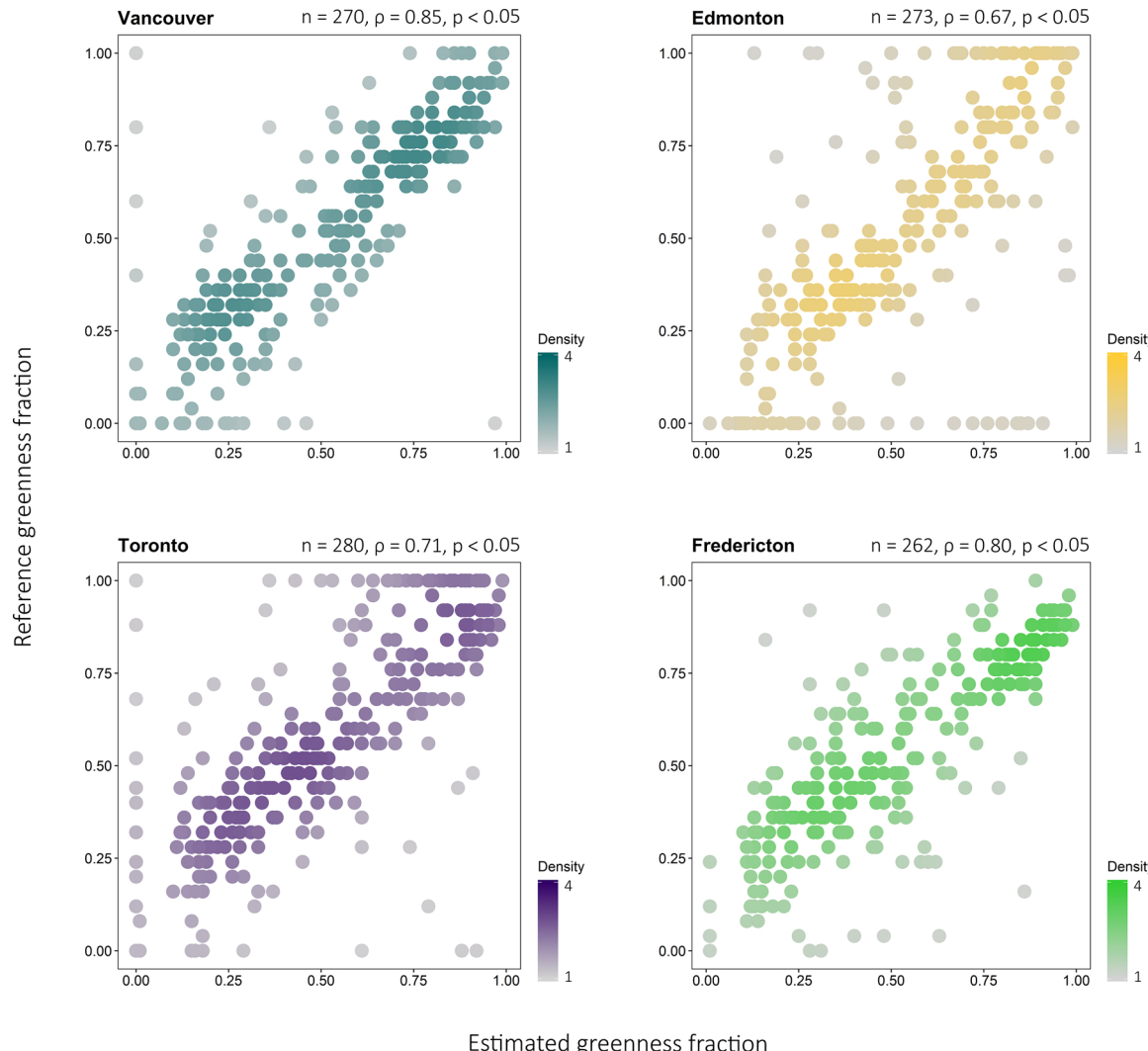


Fig. 5. Estimated (i.e. unmixed) greenness fractions plotted against reference greenness fractions, with the number of pixels (n), associated Spearman's correlation coefficient (ρ), and p-value for select years of a representative urban area of each stratum. Density indicates the amount of sample points (i.e. pixels) represented by a point on the plot.

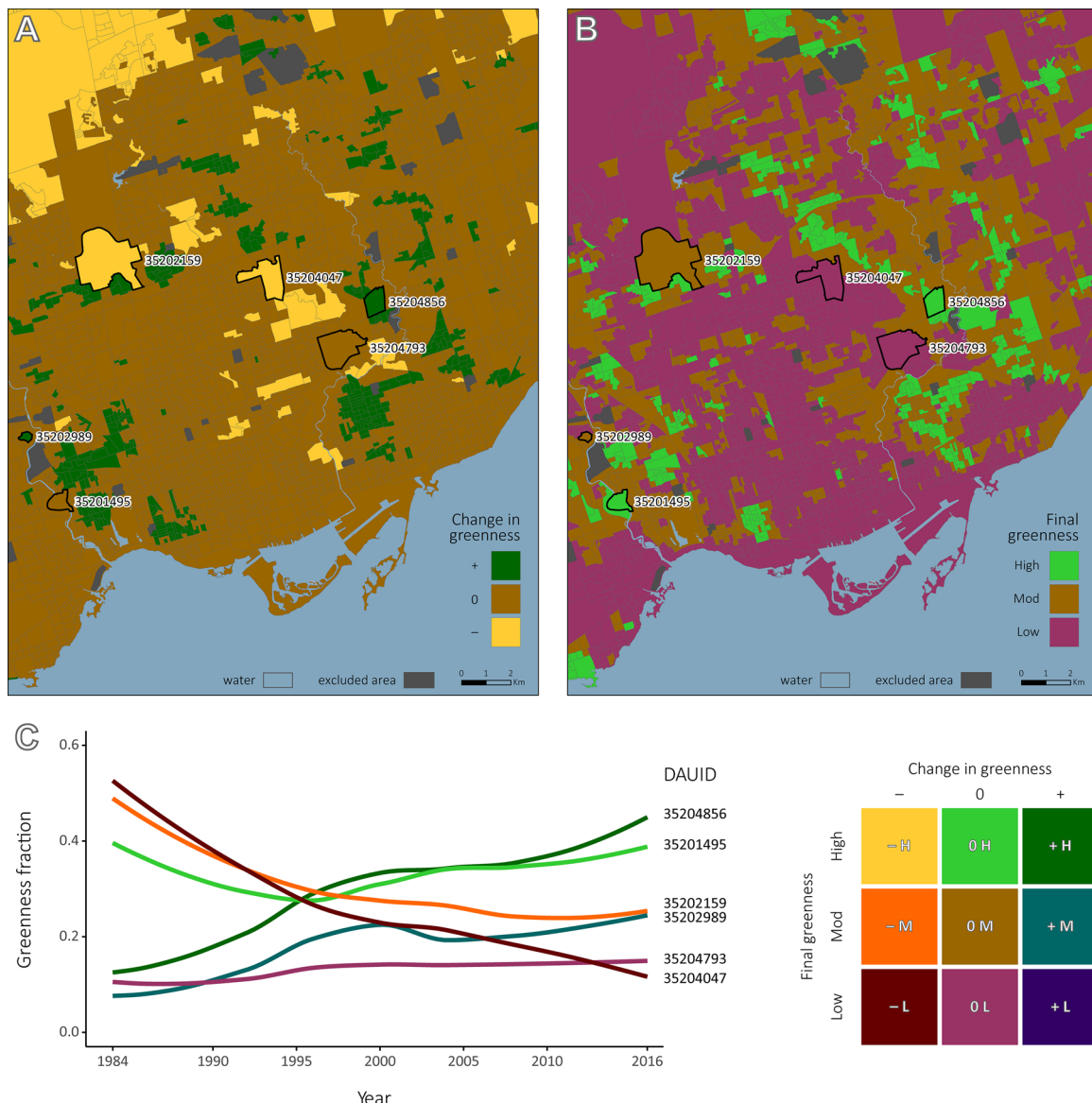


Fig. 6. Maps of greenness change (top-left panel (A)) and final greenness (top-right panel (B)) for a portion of Toronto dissemination areas (DAs). Time series of greenness fractions for select DAs (graph (C); identified by Statistics Canada census unique DA identifier code (DAUID) and outlined in black on the maps) of various urban greenness scores as distinguished by colour. A colour version of this figure is available in the online version of this article.

trends during the time series. For example, although DAs identified by unique census IDs (i.e. DAUIDs) 35202159 and 35202989 are both classified with moderate final greenness (Fig. 6B), DA 35202159 reached that state after losing greenness since 1984 (Fig. 6A), whereas DA 35202989 gained greenness (Fig. 6A). The time series of these two DAs demonstrate that despite having the same greenness level in 2016, the trajectory each DA took over the time period examined herein is markedly different (Fig. 6C).

3.3. Urban greenness score

Utilizing a multi-decadal time series of urban greenness data, the urban greenness score describes the current level of greenness in relation to its change in greenness over time using a single class. A map showing the urban greenness score for a portion of Toronto is provided as Fig. 7, indicating several DAs of different urban greenness scores. Areas that exhibited a gain in greenness and resulted in a moderate or high final level of greenness in 2016 are classified as [+ M] or [+ H], respectively (e.g. DAUID = 35202989 and 35204856 in Fig. 7),

respectively). Areas that remained with a moderate or high amount of greenness throughout the 33 years are classified as [0 M] (e.g. DAUID = 35200746 in Fig. 7) or [0 H] (e.g. DAUID = 35201495 in Fig. 7). Built-up urbanized areas that resulted in low levels of greenness in 2016, but had experienced, since 1984, an increase in greenness, are classified as [+ L] (e.g. DAUID = 35201407 in Fig. 7). Built-up areas that neither gained nor lost greenness, and generally maintained a low level of greenness are classified with the urban greenness score [0 L] (e.g. DAUID = 35204793 in Fig. 7). Areas that have lost greenness during the study time, and have resulted in either low, moderate, or high amounts of urban greenness would be classified as [- L] (e.g. DAUID = 35204047 in Fig. 7), [- M] (e.g. DAUID = 35204047 in Fig. 7), or [- H] (no example DA in Fig. 7), respectively.

3.4. Urban greenness score trends across Canada

The large area and long-term greenness time series data used in this study enabled the development of a comparative framework to be used across a range of spatial and temporal scales, as well as a national multi-

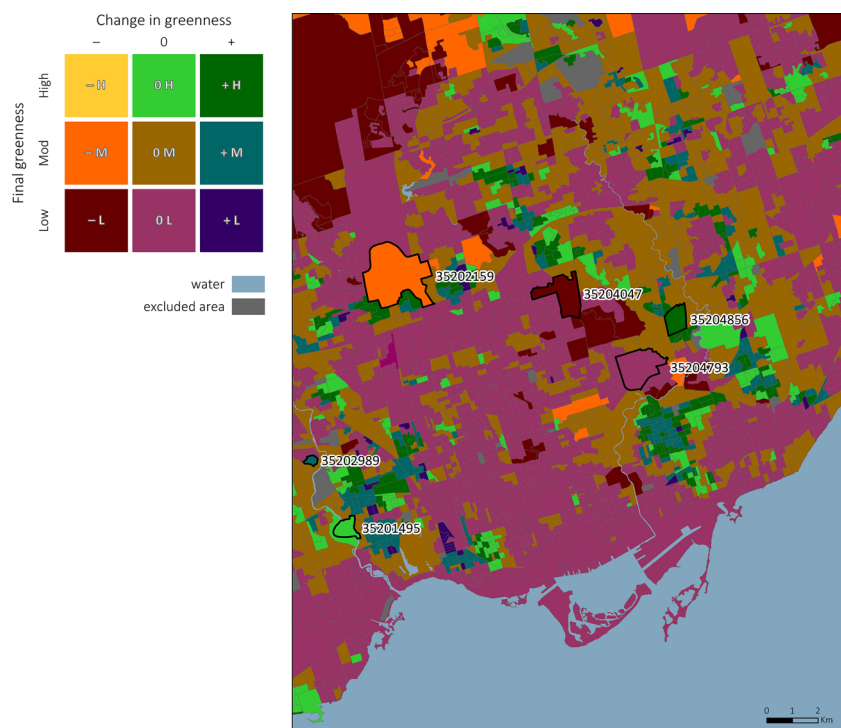


Fig. 7. Urban greenness score map for a portion of Toronto dissemination areas (DAs). Examples of each green score are identified by Statistics Canada census unique DA identifier code (DAUID) and outlined in black. A colour version of this figure is available in the online version of this article.

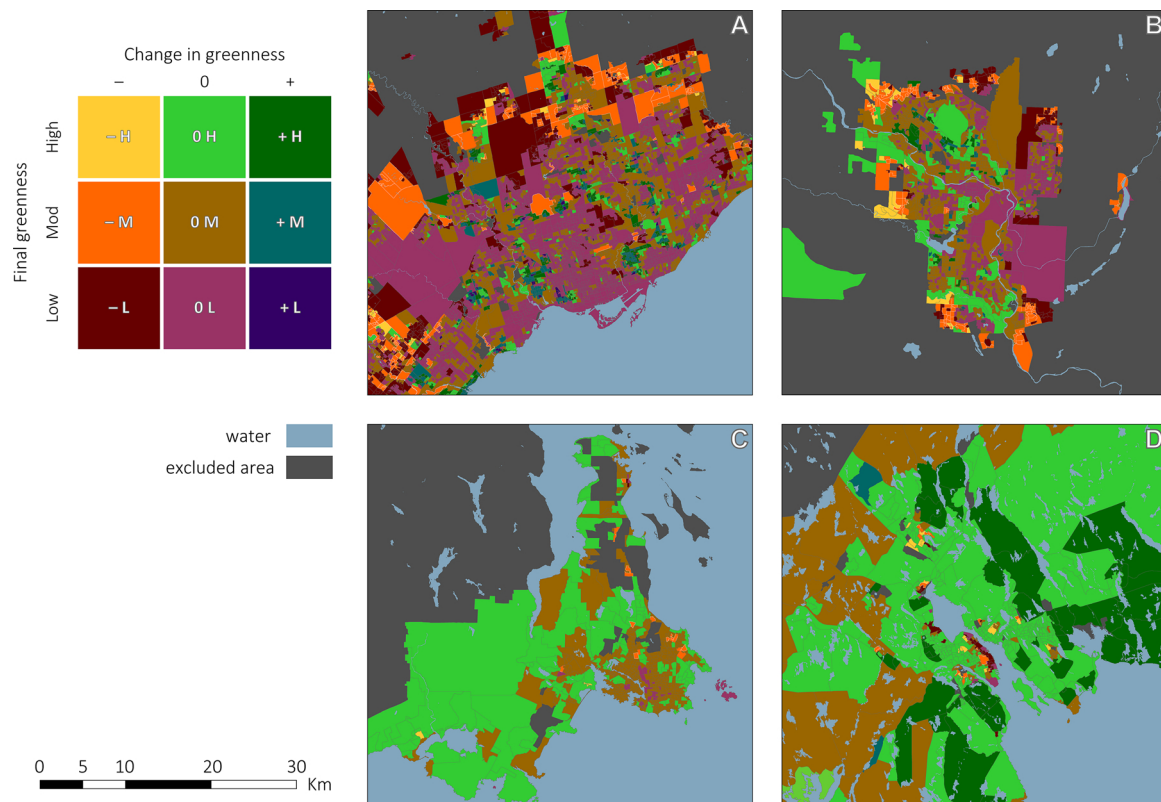


Fig. 8. Urban greenness score maps for portions of select urban areas' dissemination areas (DAs), each representing a stratum and population density group (A = Toronto (east-center stratum; high population density); B = Calgary (west-center stratum; moderately-high population density); C = Victoria (west stratum; moderately-low population density), and; D = Halifax (east stratum; low population density)). A colour version of this figure is available in the online version of this article.

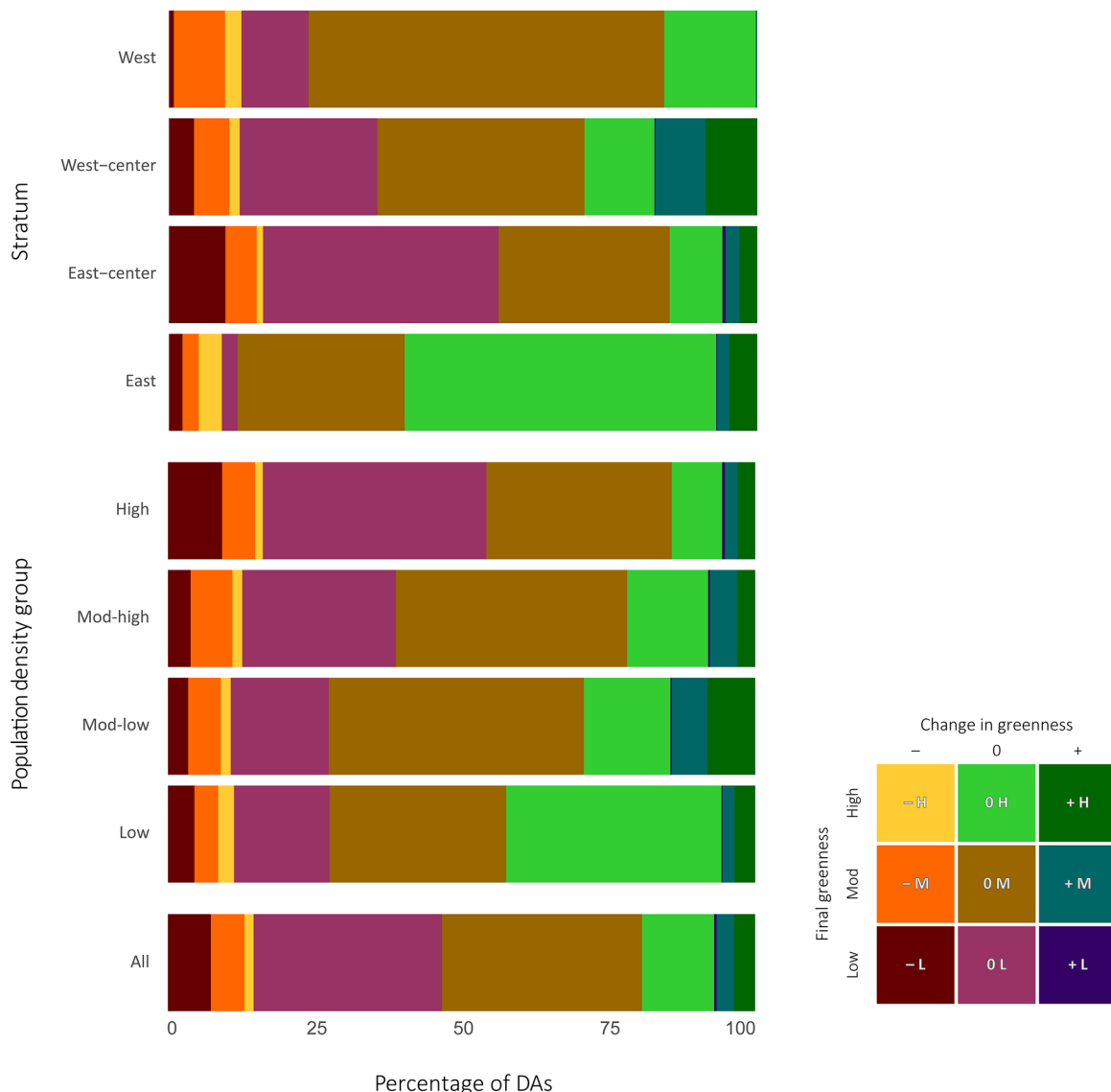


Fig. 9. Percentage of dissemination areas (DAs) classified by each urban greenness score for each stratum, population density group, as well as for all DAs. A colour version of this figure is available in the online version of this article.

decadal assessment of urban greenness. Fig. 8 shows urban greenness score maps of Toronto, Calgary, Victoria, and Halifax DAs as an example for each population density group, as well as each stratum. The distribution of urban greenness scores varied greatly between urban areas across densities and cross-continentally. For example, Victoria (Fig. 8C) and Halifax (Fig. 8D), coastal urban areas from lower population density groups, tended to have more peripheral DAs that increased or did not change in greenness and resulted in either high or moderate levels in 2016 (i.e. [+ H], [+ M], or [0 H]). The urban core of Halifax, representing the lowest population density group and the east stratum, was mostly comprised of DAs that decreased in greenness resulting in low or moderate levels in 2016 (i.e. [- L] or [- M]; Fig. 8D). In contrast, DAs in Toronto (Fig. 8A) and Calgary (Fig. 8B) that decreased or did not change in greenness and resulted in either low or high levels in 2016 (i.e. [- L], [- M], or [0 L]) were found in the urban periphery. These two densely populated urban areas are both found in Central Canada (west-center and east-center strata), which tend to be less restricted (geographically and/or legislatively) to urban spread.

The percentage of DAs classified with a given urban greenness score for each stratum, population density group, as well as for all DAs, is shown in Fig. 9. For DAs across all urban areas, most were classified as

unchanged with a moderate final level of greenness ([0 M] = 34.5 %), followed closely by those that were unchanged with a low final level of greenness ([0 L] = 30.9 %). The lowest percentage of DAs increased in greenness and resulted in a low level of greenness ([+ L] = 0.4 %). Over the 33 years, more DAs decreased in greenness ([− L] and [− M] and [− H] = 14.8 %) than increased ([+ L] and [+ M] and [+ H] = 6.9 %). Across Canada, most DAs that decreased in greenness resulted in a low level ([− L] = 7.1 %), and most that increased in greenness resulted in either a moderate or high level ([+ M] = 2.9 %, and; [+ H] = 3.6 %). Regardless of the change, most DAs exhibited a moderate or low level of greenness in 2016 (43.3% and 38.4%, respectively).

Unique distributions of urban greenness scores were evident regionally. Generally, coastal urban areas maintained the same level of greenness over the 33-year time period for the largest percentage of DAs (west = 86.5 %, and; east = 83.9 %). Moving from west to east, the proportion of unchanged, moderate level greenness decreased (i.e. [0 M]; west = 59.9 %; west-center = 36.7 %; east-center = 29.7 %, and; east = 24.7 %). Urban areas of the east-center stratum showed the largest percentage of DAs classified as no-change, low greenness ([0 L] = 39.2 %). This is demonstrated in Fig. 8A, which shows the

urban core and sprawling urban area of Toronto, much of which is classified as [0 L]. In contrast, the east strata had only a small percentage of unchanged, low greenness DAs ([0 L] = 2.8 %), distinctly lower than the percentage for DA's across all strata ([0 L] = 30.9 %). The relative lack of [0 L] in eastern urban areas is illustrated in Fig. 8D, which shows the less densely populated urban core (i.e. fewer small DAs) of Halifax and its expansive urban periphery, much of which is classified as either [0 M], [0 H], or [+ H].

The west stratum showed the lowest percentage of increased greenness scores ([+ L] and [+ M] and [+ H] = 0.3 %), whereas the west-center stratum had proportionally the most ([+ L] and [+ M] and [+ H] = 16.9 %). For the west-center's DAs classified with an increase in greenness score, most resulted in a moderate level of greenness (i.e. [+ M] = 8.2 %). In the case of decreased greenness scores, the east-center stratum had the highest percentage ([− L] and [− M] and [− H] = 16.0 %), and the east stratum the lowest ([− L] and [− M] and [− H] = 9.0 %). For the east-center's DAs classified with a decrease in greenness score, most resulted in a low level of greenness (i.e. [− L] = 9.4 %). The east stratum exhibited the most DAs with a high greenness level in 2016 (65.5 %), in relation to the remaining strata (west-center = 22.2 %; west = 21.9 %, and; east-center = 13.4 %). On the other hand, the east-center stratum had the most DAs that resulted in a low final greenness level (49.1 %) compared to the other strata (west-center = 26.4 %; west = 8.8 %, and; east = 4.9 %).

More distinct patterns in percentages of urban greenness scores are discerned between population density groups than between strata (Fig. 9). Densely populated urban areas showed the highest percentage of DAs classified as unchanged and remaining with moderate or low levels of greenness ([0 M] and [0 L] = 69.1 %; individually representing 32.3 % and 36.9 %, respectively). The percentage of these two urban greenness scores decreases as the average urban area population density decreases, whereby the low population density group exhibits only 44.0 % ([0 M] = 28.5 %, and; [0 L] = 15.5 %). In contrast, the lower the average population density of an urban area the greater percentage of DAs that maintained a high level of greenness since 1984 (low population density [0 H] = 38.8 %, and; high population density [0 H] = 9.0 %). This distinction is apparent when urban greenness score maps of Toronto (Fig. 8A, high population density) and Halifax (Fig. 8D, low population density) are compared. As seen in the figure, there is a stark contrast between Toronto's urban greenness scores [0 M] and [0 L], respectively and its relatively smaller amount of [0 H]. The opposite pattern is seen for Halifax.

Differences between population density groups were also evident between opposing changes in urban greenness scores. Densely populated urban areas, such as Toronto, showed the largest percentage of DAs that decreased in greenness ([− L] and [− M] and [− H] = 16.2 %) and the smallest percentage that increased ([+ L] and [+ M] and [+ H] = 5.6 %). In the case of decreased greenness in high population density urban areas, most DAs resulted in a low level of greenness ([− L] = 9.0 %). On the other hand, the greatest percentage of DAs that increased in greenness were found in moderately-low population density urban areas, such as Victoria ([+ L] and [+ M] and [+ H] = 14.1 %), as well as the smallest percentage that decreased in greenness ([− L] and [− M] and [− H] = 11.2 %). In the case of increased greenness in moderately-low population density urban areas, most DAs resulted in a high level of greenness ([+ H] = 7.9 %). Halifax and other urban areas of the low population density group showed the largest percentage of DAs that decreased in greenness and still resulted in high levels of greenness ([− H] = 2.6 %), whereas Toronto and other densely populated urban areas showed the smallest percentage ([− H] = 1.5 %). Conversely, urban areas with a high population density had the largest percentage of DAs classified as increased, low final level of greenness ([+ L] = 0.5 %), whereas low population density urban areas had the smallest ([+ L] = 0.1 %). Of all the population density groups, the moderately-high population density group showed the largest percentage of DAs classified as a decrease in greenness that resulted in a

moderate level ([− M] = 7.6 %), and the low population density group showed the smallest ([− M] = 4.4 %). For the case of a greenness increase that resulted in a moderate greenness level, DAs of moderately-low population density urban areas had the most ([+ M] = 6.1 %), but both the high and low population density groups had the least ([+ M] = 2.1 % and 1.9 %, respectively). Low population density urban areas exhibited the most DAs that resulted in a high final greenness level (45.2 %), in relation to the remaining population density groups (moderately-low = 25.1 %; moderately-high = 19.6 %, and; high = 13.6 %). Conversely, densely populated urban areas presented the most DAs with a low level of greenness in 2016 (46.3 %) compared to the other population density groups (moderately-high = 29.0 %; low = 20.1 %, and; moderately-low = 19.0 %).

4. Discussion

We developed a satellite time series based, urban greenness score, from which insights were gained about the current state of urban greenness and how it has changed since the mid-1980s. The score was developed across 18 select major Canadian urban areas, as well as between four geographic regions and four population density groups. Across the urban areas, we found an overall loss in greenness from 1984 to 2016 (15 % of DAs) that resulted in an overall moderate level of greenness (~20 % – 40 %) in the terminal year of our analysis (2016). Distinctions in urban greenness score distributions between urban areas of different population densities (in 2016) indicate that urban development patterns play a large role in influencing Canadian urban greenness availability. Additionally, differences in urban greenness score distributions between geographic regions indicate that dominant regional vegetation types may also contribute to urban greenness dynamics. Urban areas with the highest average population densities in 2016 had the largest proportion of DAs that experienced a loss in greenness, whereas moderately-low population density urban areas had the largest proportion of DAs that increased in greenness during the time period. Of all DAs that experienced an increase in greenness, most resulted in a high level of greenness in 2016. Nationally, greenness loss most often occurred in areas with urban expansion or infilling. However, since urban areas are complex networks of multiple municipalities with varying land uses and urban policies, it is not appropriate to imply overarching influences on urban greenness trends. The data generation through the methods demonstrated in this analysis, including the development of the urban greenness score framework, allows for individual urban area analyses of urban greenness trends and potential factors involving policy, socio-economics, and/or the built environment.

4.1. Analysis approach

The urban greenness score developed in this analysis, using final greenness and the TS-derived overall change in greenness, provides a new framework for urban change and is suitable to apply across spatial levels, such as at the DA level or on a national scale. Depending on the year from which greenness data is derived, the urban greenness score can be tuned to relate to a different greenness state within the time series. If greenness information from the initial year was used, the urban greenness score would show how the quantity of urban vegetation has changed since the start of the time series. Although this provides an interesting glimpse into the past, planners and developers require accessible and relevant data in order to prioritize goals and allocate resources efficiently and effectively for long-term strategic plans (Haaland and Konijnendijk van den Bosch, 2015). The final level of greenness from a time series presents the most up-to-date information that enables urban planners to better understand current green areas and their recent histories. As greenness data continues to be collected, the urban greenness score can be updated accordingly and comparisons between iterations would inform about potential shifts in

single-year greenness, as well as its on-going trends. Additionally, since the urban greenness score was developed using administrative boundaries (census DAs), investigations using additional municipal, regional, or census data with the urban greenness score may help illuminate potential factors influencing urban greenness losses or gains.

Our developed urban greenness score simply yet thoroughly describes urban greenness and its change over time. Prior to the availability of dense time series data, standard practice for trend analysis considered the relative change of values extracted from satellite imagery of different times. However, as relative change only considers data from two time steps, it does not harness the full potential of long, high frequency time series data that are currently available. In addition, relative change analyses may skew results in favour of anomalies found in the initial and/or final years. Instead, TS-derived change, as used in the urban greenness score, is robust against outliers and uneven non-normal distributions of input data as it is computed using pairwise slopes between all of the time series data points (Ohlson et al., 2015; Wilcox, 2010). Due to these advantages TS has become a common method for quantifying change of remotely sensed data (Fernandes and Leblanc, 2005; Liu et al., 2015; Mishra and Mainali, 2017), and is particularly beneficial for a high-frequency, multi-decadal urban land dynamics characterization framework such as the urban greenness score.

Spectral unmixing successfully captured the level of urban greenness across 18 urban areas in four Canadian geographic-based strata. From the validation procedure, the estimated greenness fractions largely correlated with the reference greenness fractions derived from imagery in Google Earth. All cities had rank correlation coefficients (ρ) > 0.70 except for Edmonton ($\rho = 0.67$). Lower correlations between estimated and reference greenness fractions can be attributed to some spatial and temporal mismatch as a result of comparing imagery of different sources. Despite careful spatial alignment of estimated Landsat-based greenness fraction data with reference Google Earth imagery, some pixel misregistration is a common, yet minor, source of error. Although both Landsat and Google Earth imagery used in this analysis were acquired during the growing season of the same year, a maximum two-month temporal mismatch between estimated and reference data was still possible. For example, Edmonton's lower correlation may be due to temporal mismatch of imagery combined with the phenology of herbaceous vegetation typically found in the prairie ecozone (i.e. west-center stratum; Rochon et al., 2010). The phenology of herbaceous vegetation that thrives in this geographic region, particularly grasses, is closely related to drought conditions that advance senescence and loss of greenness (Cui et al., 2017). It may be the case that Landsat and Google Earth imagery were acquired at a large enough temporal gap that the discrepancy in phenology contributed to inconsistencies between estimated and reference greenness fractions. It may also be the case that real changes in greenness occurred during the temporal gap between data from Landsat and Google Earth Imagery, such as greenness loss due to construction. Some inaccuracy in estimated greenness fractions can also be attributed to the dark end-member chosen for the spectral unmixing technique, particularly for densely forested pixels such as those found in the west stratum. However, these pixels tend to be found in peripheral DAs and thus should not greatly influence the average trend of the entire urban area. Since we conducted the validation procedure for a representative urban area of each geographic stratum, the remaining urban areas would show similar high correlations between estimated and reference greenness fractions.

4.2. Urban greenness score trends across Canada

In this analysis we compare over 30 years of satellite data systematically across major Canadian urban centers to spatially identify and temporally characterize urban greenness both geographically and by population density. Overall, our results correspond with studies

examining how greenness of various Canadian and international cities has changed within the past quarter century. For example, our results are in line with those of Jin et al. (2019), who indicated that three of five selected North American cities (all found on the western half) experienced greenness loss between 1992 and 2011. In the same study, four of nine Asian cities also showed a negative temporal trend of greenness, whereas the two major Australian cities investigated (Melbourne and Sydney) indicated an increase in greenness. Kabisch and Haase (2013) found that European cities have also experienced greening trends (between 1990 and 2006), with variations between cities of different climatic regions (i.e. western, eastern, southern, and northern Europe). Similar to McGovern and Pasher (2016), who found that the national urban tree canopy did not substantially change between 1990 and 2012, we can conclude that, on average, Canadian urban areas maintained a similar level of greenness between 1984 and 2016.

McGovern and Pasher (2016) found a similar trend in urban tree canopy loss by Canadian ecozones between 1990 and 2012, where the majority of loss (6 %) occurred in the Ontario mixedwoods and British Columbia Pacific maritime regions. In our analysis, the east-center stratum (which would include most of Ontario's mixedwoods ecozone) only experienced a marginal greenness loss, and the west coast urban areas (which would be part of the British Columbia Pacific maritime ecozone) did not show much more greenness loss than the other geographic regions. Alternatively, we found for both Vancouver and Victoria (west stratum) that recent greenness levels were relatively high despite an overall loss since 1992, in agreement with the findings by Jin et al. (2019). The high incidence of peripheral areas that decreased in greenness in our study is similar to the findings of McGovern and Pasher (2016), who noted that the loss of urban tree canopy in Ontario was predominantly a result of continued urban expansion. For both studies the greatest increase in greenness was found in Prairie urban areas (i.e. west-center stratum), which are relatively younger cities since early settlement in this region heavily focused on the development of agriculture in rural areas (Thomas, 1975). As Prairie cities are younger, with low population densities, and have not undertaken much urban infilling, the time series of satellite imagery used in this analysis captured their sustained green-up.

In densely populated urban areas, our study identified only 6 % of DAs that increased in greenness, but just over 16 % of DAs that showed the largest reduction in greenness. This pattern may be present because Canadian cities are much younger and with relatively lower urban densities than many other cities internationally. Only since the mid-1970s, Toronto and other industrialized Canadian cities turned to the urban periphery to expand industrial and commercial facilities, leaving open lots in the urban core available for development (Gertler, 1995). By the mid- to late-1990s many of these cities took action to remediate these abandoned lots and develop them residentially and/or commercially, and only in some cases into public green spaces (De Sousa, 2002). Now, as the urban core is relatively stable, development of Canadian cities most often occurs along the urban fringe where space is available.

Areas that lost greenness between 1984 and 2016 within the metropolises of Toronto, Vancouver, and Montréal were mostly located at the urban edges, which agrees with previous work that has noted the trade-off between urban greenness and expansion around the periphery of cities around the world (Catalán et al., 2008; Jin et al., 2019; Zhao et al., 2016). Despite the consistent loss of greenness occurring in the urban periphery, many areas on the edge of the urban landscape exhibited higher levels of greenness by the end of the analysis period than those deeper within the core. It is possible that recent urban developments have adopted a greater focus on integrating green spaces into their plans. This result of recent urban development greening is in line with others who have accounted the increased presence of urban vegetation moving away from the core of many Asian cities (Jin et al., 2019), as well as the metropolitan area of Vancouver (Jarvis et al.,

2020). Ultimately, the noted green-up trends following new urban expansion projects across Canada, as well as globally, point towards urban greenness trends acting as a function of inherent urban form.

Greening international cities, identified by Jin et al. (2019), also maintained medium-dense vegetation cover while North American cities in the same study that lost greenness overall were unable to maintain their medium-dense vegetation. Our results translate to a similar conclusion; DAs that lost greenness typically resulted in low greenness levels in 2016, whereas those that gained greenness attained high levels. Yet, the DAs in high population density urban areas of our study that gained greenness over the 33 years for the most part resulted in high levels of greenness in 2016. These areas are found interspersed in the urban fabric, such as those just outside Toronto's core, which implies that the complexity of intra-urban greenness dynamics may be influenced by several factors, likely including but not limited to municipal and/or regional planning, demand for densification, and/or individual homeowner decision making.

4.3. Strengths and limitations

We offer a novel and manageable characterization framework of urban change using the urban greenness score, developed using regionally specific spectrally unmixed vegetation greenness across major Canadian urban areas and over three decades. Our results show major trends of urban greenness over 30 years, particularly a greater increase in the Prairies than in Ontario, and greater declines in greenness in denser urban areas. However, urban greenness dynamics are closely linked to historical and on-going place-based land use factors (Chauvin et al., 2017; Deininger and Binswanger, 1999; Özgüler, 2011; Zhao et al., 2015). For example, McGovern and Pasher (2016) indicate that Canadian urban trees were typically lost as a result of infilling or expansion, but in some cases urban tree canopy also increased alongside tree planting initiatives of new developments. In another case, in which urban areas were surrounded by agriculture, the same authors noted that the conversion of these lands into suburban housing translated into the addition of tree cover. This pattern may be persistent in the Prairies and may help explain its substantial urban greenness growth over the past few decades as identified by McGovern and Pasher (2016) as well as this study. Continued work about urban greenness trends in Canada should investigate relative association with governance and socio-economic factors, such as land use policies, urban planning, wealth, housing types, and prices (as identified previous by Lepczyk et al. (2017), as well as investigate specific cases of greening policies that may be key to long-term urban vegetation dynamics.

This paper provides a foundational characterization of urban greenness with an opportunity to better understand how differences in contemporary greenness and its temporal dynamics vary nationally between urban areas (of different geographic regions and population densities), within urban areas on detailed administrative level (DA in the case of Canada), as well as nationally across all urban DAs. Our results show that summarizing spectrally unmixed vegetation greenness data on the DA level retains nuances from the pixel level data but provides a practical approach for further applications. As this analysis focused on the quantification of urban greenness, key elements in assessing the success of urban green spaces, including but not limited to vegetation type and quality, ecosystem services, accessibility, and user experiences, were not considered. For example, greenness of private urban green spaces was not distinguished, but would be crucial in green space equity analysis.

The utilization of the open Landsat archive in this work provides insights into long-term patterns of urbanization and promotes development of an index of general utility both within and outside of the remote sensing community. As we have presented in this paper, the unique combination of fine spatial detail and high temporal resolution of the Landsat imagery enables temporal assessments of individual urban areas that can be conducted systematically, transparently,

efficiently, and at a relatively low cost. Using the Landsat-derived urban greenness score, residents, urban planners, and developers are able to rapidly understand multi-decadal and detailed spatial patterns of urban vegetation. These patterns can be further explored with focused analyses using the original spectrally unmixed greenness fraction input data. In addition, the greenness score provides a useful tool for immediate implementation in interdisciplinary research, including epidemiological studies analyzing changes in health status related to variation in urban vegetation. The fusion of open access remotely sensed data and an operational urban greenness score as presented in this paper provides decision makers with otherwise unavailable information for strategic, evidence-based, and sustainable urban policies.

5. Conclusion

The findings of this research highlight the successful application of moderate-resolution satellite image time series data in an analysis of greenness trends over three decades for the largest cities and provincial capitals across Canada, in which over half of the country's population reside, and covering an area greater than 40,000 km². Our novel urban greenness score presented herein, incorporates change in greenness (derived from the Theil-Sen estimator) with final greenness at the end of the time series, and is a robust and applicable method for continued urban monitoring—a key requirement for long-term planning. Using this urban greenness score to characterize the trend in greenness of 18 Canadian urban areas, we found that most areas have maintained stable amounts of greenness since 1984. Overall, most DAs across Canada maintained a moderate or low level of greenness between 1984 and 2016. More DAs decreased than increased in greenness, as most DAs that gained greenness resulted in a moderate or high level, whereas those that lost greenness mostly resulted in a low level. Intra-urban spatial trends in greenness were noted across cities of different geographic regions and average population densities, whereas low greenness levels typically occurred in urban cores and losses in greenness commonly occurred in areas with urban development and expansion. The east coast remained the greenest over the 33 years, and the Prairies (east-center stratum) experienced the most urban greenness increases. Urban areas with a moderately-low population density gained the most greenness, whereas densely populated urban areas experienced the most loss. Despite general patterns in intra-urban greenness, each urban area exhibited a unique distribution of urban greenness scores that speaks to the inherent complexity of current and historical land uses and urban policies. The urban greenness score framework and unprecedented 33-year urban greenness score data for 18 major Canadian urban areas produced in this study enable continued investigation into urban greenness across Canada, such as the spatial and temporal relationships between greenness and other urban-related factors to provide a greater understanding for planning equitable and sustainable green spaces.

CRediT authorship contribution statement

Agatha Czekajlo: Conceptualization, Methodology, Software, Formal analysis, Data curation, Writing - original draft, Writing - review & editing, Visualization, Project administration. **Nicholas C. Coops:** Conceptualization, Methodology, Writing - review & editing, Supervision, Project administration, Funding acquisition. **Michael A. Wulder:** Conceptualization, Methodology, Writing - review & editing, Supervision, Funding acquisition. **Txomin Hermosilla:** Methodology, Software, Resources, Writing - review & editing. **Yuhao Lu:** Software, Validation, Resources, Writing - review & editing. **Joanne C. White:** Methodology, Writing - review & editing, Supervision. **Matilda van den Bosch:** Writing - review & editing, Supervision, Funding acquisition.

Declaration of Competing Interest

The authors declare that they have no known competing financial interests or personal relationships that could have appeared to influence the work reported in this paper.

Acknowledgements

This research was undertaken as part of the “Earth Observation to Inform Canada’s Climate Change Agenda (EO3C)” project jointly funded by the Canadian Space Agency (CSA), Government Related Initiatives Program (GRIP), and the Canadian Forest Service (CFS) of Natural Resources Canada (NRCan). Support also provided by a NSERC Discovery grant to Coops, and by a Canadian Institutes of Health Research (CIHR) grant to van den Bosch (project grant reference number 156152). This research was enabled in part by capacity provided by WestGrid (www.westgrid.ca) and Compute Canada (www.computecanada.ca). Open access is supported by the Government of Canada. We thank Marco Sanelli for help with the validation procedure.

References

- Anchang, J.Y., Ananga, E.O., Pu, R., 2016. An efficient unsupervised index based approach for mapping urban vegetation from IKONOS imagery. *Int. J. Appl. Earth Obs. Geoinf.* 50, 211–220. <https://doi.org/10.1016/j.jag.2016.04.001>.
- Angel, S., Parent, J., Civco, D.L., Blei, A., Potere, D., 2011. The dimensions of global urban expansion: estimates and projections for all countries, 2000–2050. *Prog. Plann.* 75, 53–107. <https://doi.org/10.1016/j.progress.2011.04.001>.
- Asner, G.P., Heidebrecht, K.B., 2002. Spectral unmixing of vegetation, soil and dry carbon cover in arid regions: comparing multispectral and hyperspectral observations. *Int. J. Remote Sens.* 23, 3939–3958. <https://doi.org/10.1080/01431160110115960>.
- Atasoy, M., 2018. Monitoring the urban green spaces and landscape fragmentation using remote sensing: a case study in Osmaniye, Turkey. *Environ. Monit. Assess.* 190, 713. <https://doi.org/10.1007/s10661-018-7109-1>.
- Bateson, A., Curtiss, B., 1996. A method for manual endmember selection and spectral unmixing. *Remote Sens. Environ.* 55, 229–243. [https://doi.org/10.1016/S0034-4257\(95\)00177-8](https://doi.org/10.1016/S0034-4257(95)00177-8).
- Block, E.P., Zimmerman, F.J., Aguilar, E., Stanley, L., Halfon, N., 2018. Early child development, residential crowding, and commute time in 8 US states, 2010–2017. *Am. J. Public Health* 108, 1550–1557. <https://doi.org/10.2105/AJPH.2018.304680>.
- Boardman, J.W., 1993. Automating Spectral Unmixing of AVIRIS Data Using Convex Geometry Concepts.
- Boardman, J.W., Kruse, F.A., Green, R.O., 1995. Mapping Target Signatures via Partial Unmixing of AVIRIS Data.
- Breuecker, J.K., Fansler, D.A., 1983. The economics of urban sprawl: theory and evidence on the spatial sizes of cities. *Rev. Econ. Stat.* 65, 479. <https://doi.org/10.2307/1924193>.
- Catalán, B., Saurí, D., Serra, P., 2008. Urban sprawl in the Mediterranean? Patterns of growth and change in the Barcelona Metropolitan Region 1993–2000. *Landscape Urban Plan.* 85, 174–184. <https://doi.org/10.1016/j.landurbplan.2007.11.004>.
- Chauvin, J.P., Glaeser, E., Ma, Y., Tobio, K., 2017. What is different about urbanization in rich and poor countries? Cities in Brazil, China, India and the United States. *J. Urban Econ.* 98, 17–49. <https://doi.org/10.1016/j.jue.2016.05.003>.
- Cleveland, W.S., Devlin, S.J., 1988. Locally weighted regression: an approach to regression analysis by local fitting. *J. Am. Stat. Assoc.* 83, 596–610. <https://doi.org/10.1080/01621459.1988.10478639>.
- Core Team, R., 2018. R: a Language and Environment for Statistical Computing.
- Coulson, M.R.C., 1987. In the matter of class intervals for choroplethic maps: with particular reference to the work of George F Jenks. *Cartogr. Int. J. Geogr. Inf. Geovisualization* 24, 16–39. <https://doi.org/10.3138/u7x0-1836-5715-3546>.
- Cui, T., Martz, L., Guo, X., 2017. Grassland phenology response to drought in the Canadian Prairies. *Remote Sens.* 9, 1258. <https://doi.org/10.3390/rs9121258>.
- De Sousa, C.A., 2002. Measuring the public costs and benefits of brownfield versus Greenfield development in the greater Toronto area. *Environ. Plan. B Plan. Des.* 29, 251–280. <https://doi.org/10.1068/b1283>.
- Deininger, K., Binswanger, H., 1999. The evolution of the World Bank's land policy: principles, experience, and future challenges. *World Bank Res. Obs.* 14, 247–276. <https://doi.org/10.1093/wbro/14.2.247>.
- Fernandes, R., Leblanc, S.G., 2005. Parametric (modified least squares) and non-parametric (Theil-Sen) linear regressions for predicting biophysical parameters in the presence of measurement errors. *Remote Sens. Environ.* 95, 303–316. <https://doi.org/10.1016/j.rse.2005.01.005>.
- Fragkias, M., Güneralp, B., Seto, K.C., Goodness, J., 2013. A Synthesis of Global Urbanization Projections, in: Urbanization, Biodiversity and Ecosystem Services: Challenges and Opportunities. Springer Netherlands, Dordrecht, pp. 409–435. https://doi.org/10.1007/978-94-007-7088-1_21.
- Fung, T., Siu, W.-L., 2001. A study of green space and its changes in Hong Kong Using NDVI. *Geogr. Environ. Model.* 5, 111–122. <https://doi.org/10.1080/13615930120086032>.
- Gertler, M., 1995. Adapting to New Realities: Industrial Land Outlook for Metropolitan Toronto, Durham, York, Halton, Peel, Hamilton-Wentworth and Waterloo. Berridge Lewinberg Greenberg Dark Gabor Ltd., Municipality of Metropolitan Toronto, Toronto.
- Glaeser, E.L., Kahn, M.E., 2003. Sprawl and urban growth. *SSRN Electron. J.* <https://doi.org/10.2139/ssrn.405962>.
- Green, A.A., Berman, M., Switzer, P., Craig, M.D., 1988. A transformation for ordering multispectral data in terms of image quality with implications for noise removal. *IEEE Trans. Geosci. Remote. Sens.*
- Haaland, C., Konijnendijk van den Bosch, C., 2015. Challenges and strategies for urban green-space planning in cities undergoing densification: a review. *Urban For. Urban Green.* 14, 760–771. <https://doi.org/10.1016/j.ufug.2015.07.009>.
- Haase, D., Jänicke, C., Wellmann, T., 2019. Front and back yard green analysis with subpixel vegetation fractions from earth observation data in a city. *Landscape Urban Plan.* 182, 44–54. <https://doi.org/10.1016/j.landurbplan.2018.10.010>.
- Hartig, T., Mitchell, R., de Vries, S., Frumkin, H., 2014. Nature and health. *Annu. Rev. Public Health* 35, 207–228. <https://doi.org/10.1146/annurev-publhealth-032013-182443>.
- Hermosilla, T., Wulder, M.A., White, J.C., Coops, N.C., Hobart, G.W., 2018. Disturbance-informed annual land cover classification maps of Canada's forested ecosystems for a 29-year landsat time series. *Can. J. Remote Sens.* 44, 67–87. <https://doi.org/10.1080/07038992.2018.1437719>.
- Heynen, N., Perkins, H.A., Roy, P., 2006. The political ecology of uneven urban green space. *Urban Aff. Rev.* 42, 3–25. <https://doi.org/10.1177/1078087406290729>.
- Hayday, J.T., Ridwan, M., 2018. Assessment of the quality of public Green Open Space (GOS) in the urban fringes in response to urban sprawl phenomenon (case study District of Tanah Sareal, Bogor City). *IOP Conf. Ser. Earth Environ. Sci.* 179, 012027. <https://doi.org/10.1088/1755-1315/179/1/012027>.
- Jarvis, I., Gergel, S., Koehoorn, M., van den Bosch, M., 2020. Greenspace access does not correspond to nature exposure: measures of urban natural space with implications for health research. *Landscape Urban Plan.* 194. <https://doi.org/10.1016/j.landurbplan.2019.103686>.
- Jassby, A.D., Cloern, J.E., 2017. Wq: Some Tools for Exploring Water Quality Monitoring Data.
- Jenks, G.F., Caspall, F.C., 1971. Error on choroplethic maps: definition, measurement, reduction. *Ann. Assoc. Am. Geogr.* 61, 217–244. <https://doi.org/10.1111/j.1467-8306.1971.tb00779.x>.
- Jin, J., Gergel, S.E., Lu, Y., Coops, N.C., Wang, C., 2019. Asian cities are greening while some North American cities are browning: long-term greenspace patterns in 16 cities of the pan-Pacific region. *Ecosystems* 1–17. <https://doi.org/10.1007/s10021-019-00409-2>.
- Kabisch, N., Haase, D., 2013. Green spaces of European cities revisited for 1990–2006. *Landscape Urban Plan.* 110, 113–122. <https://doi.org/10.1016/j.landurbplan.2012.10.017>.
- Krefis, A., Augustin, M., Schlünzen, K., Oßenbrügge, J., Augustin, J., 2018. How does the urban environment affect health and well-being? A systematic review. *Urban Sci.* 2, 21. <https://doi.org/10.3390/urbansci2010021>.
- Kulish, M., Richards, A., Gillitzer, C., 2012. Urban structure and housing prices: some evidence from Australian cities. *Econ. Rec.* 88, 303–322. <https://doi.org/10.1111/j.1475-4932.2012.00829.x>.
- Kumagai, K., 2011. Verification of the analysis method for extracting the spatial continuity of the vegetation distribution on a regional scale. *Comput. Environ. Urban Syst.* 35, 399–407. <https://doi.org/10.1016/j.compenvurbsys.2011.05.005>.
- Landry, S.M., Chakraborty, J., 2009. Street trees and equity: evaluating the spatial distribution of an urban Amenity. *Environ. Plan. A Econ. Sp.* 41, 2651–2670. <https://doi.org/10.1068/a41236>.
- Lepczyk, C.A., Aronson, M.F.J., Evans, K.L., Goddard, M.A., Lerman, S.B., Macivor, J.S., 2017. Biodiversity in the city: fundamental questions for understanding the ecology of urban green spaces for biodiversity conservation. *Bioscience*. <https://doi.org/10.1093/biosci/bix079>.
- Li, W., Saphores, J.-D.M., Gillespie, T.W., 2015. A comparison of the economic benefits of urban green spaces estimated with NDVI and with high-resolution land cover data. *Landscape Urban Plan.* 133, 105–117. <https://doi.org/10.1016/J.LANDURBPLAN.2014.09.013>.
- Liu, X., Kafatos, M., 2007. Land-cover mixing and spectral vegetation indices. *Int. J. Remote Sens.* <https://doi.org/10.1080/01431160500056907>.
- Liu, Y., Wang, Y., Peng, J., Du, Y., Liu, X., Li, S., Zhang, D., 2015. Correlations between urbanization and vegetation degradation across the world's metropolises using DMSP/OLS nighttime light data. *Remote Sens.* 7, 2067–2088. <https://doi.org/10.3390/rs70202067>.
- Livesley, S.J., McPherson, G.M., Calfapietra, C., 2016. The urban forest and ecosystem services: impacts on urban water, heat, and pollution cycles at the tree, street, and city scale. *J. Environ. Qual.* 45, 119–124. <https://doi.org/10.2134/jeq2015.11.0567>.
- Lu, D., Weng, Q., 2006. Use of impervious surface in urban land-use classification. *Remote Sens. Environ.* 102, 146–160. <https://doi.org/10.1016/J.RSE.2006.02.010>.
- Lu, Y., Coops, N.C., Hermosilla, T., 2017. Estimating urban vegetation fraction across 25 cities in pan-Pacific using Landsat time series data. *ISPRS J. Photogramm. Remote Sens.* 126, 11–23. <https://doi.org/10.1016/j.isprsjprs.2016.12.014>.
- Marshall, I.B., Schut, P.H., Ballard, M., 1999. A national ecological framework for Canada: attribute data. *Ottawa/Hull*.
- McGovern, M., Pasher, J., 2016. Canadian urban tree canopy cover and carbon sequestration status and change 1990–2012. *Urban For. Urban Green.* 20, 227–232. <https://doi.org/10.1016/j.ufug.2016.09.002>.
- Mishra, N.B., Mainali, K.P., 2017. Greening and browning of the Himalaya: spatial patterns and the role of climatic change and human drivers. *Sci. Total Environ.* 587–588, 326–339. <https://doi.org/10.1016/j.scitotenv.2017.02.156>.

- Müllner, D., 2013. Fastcluster: fast hierarchical, agglomerative clustering routines for r and Python. *J. Stat. Softw.* 53, 1–18. <https://doi.org/10.18637/jss.v053.i09>.
- Muzet, A., 2007. Environmental noise, sleep and health. *Sleep Med. Rev.* <https://doi.org/10.1016/j.smrv.2006.09.001>.
- Ohlson, James A., Kim, Seil, Ohlson, J.A., Kong, C., Kim, S., 2015. Linear valuation without OLS: the Theil-Sen estimation approach. *Rev Acc. Stud* 20, 395–435. <https://doi.org/10.1007/s11142-014-9300-0>.
- Okujeni, A., van der Linden, S., Tits, L., Somers, B., Hostert, P., 2013. Support vector regression and synthetically mixed training data for quantifying urban land cover. *Remote Sens. Environ.* 137, 184–197. <https://doi.org/10.1016/j.rse.2013.06.007>.
- Özgürer, H., 2011. Cultural differences in attitudes towards urban parks and green spaces. *Landscape Res.* 36, 599–620. <https://doi.org/10.1080/01426397.2011.560474>.
- Patino, J.E., Duque, J.C., 2013. A review of regional science applications of satellite remote sensing in urban settings. *Comput. Environ. Urban Syst.* 37, 1–17. <https://doi.org/10.1016/J.COMENVURBSYS.2012.06.003>.
- Phinn, S., Stanford, M., Scarth, P., Murray, A.T., Shyy, P.T., 2002. Monitoring the composition of urban environments based on the vegetation-impermeable surface-soil (VIS) model by subpixel analysis techniques. *Int. J. Remote Sens.* 23, 4131–4153. <https://doi.org/10.1080/01431160110114998>.
- Powell, R.L., Roberts, D.A., 2008. Characterizing Variability of the Urban Physical Environment for a Suite of Cities in Rondônia, Brazil. *Earth Interact.* 12, 1–32. <https://doi.org/10.1175/2008EI246.1>.
- Powell, R.L., Roberts, D.A., 2010. Characterizing urban land-cover change in Rondônia, Brazil: 1985 to 2000. *J. Lat. Am. Geogr.* 9, 183–211.
- Rochon, C., Smith, R.B., Hayes, T., 2010. Canadian Biodiversity: Ecosystem Status and Trends 2010.
- Ruiz, L.A., Recio, J.A., Fernández-Sarría, A., Hermosilla, T., 2011. A feature extraction software tool for agricultural object-based image analysis. *Comput. Electron. Agric.* 76, 284–296. <https://doi.org/10.1016/J.COMPAG.2011.02.007>.
- Saiz, A., 2010. The geographic determinants of housing supply. *Q. J. Econ.* 125, 1253–1296. <https://doi.org/10.1162/qjec.2010.125.3.1253>.
- Schneider, A., 2012. Monitoring land cover change in urban and peri-urban areas using dense time stacks of Landsat satellite data and a data mining approach. *Remote Sens. Environ.* 124, 689–704. <https://doi.org/10.1016/j.rse.2012.06.006>.
- Schneider, A., Friedl, M.A., Potere, D., 2009. A new map of global urban extent from MODIS satellite data. *Environ. Res. Lett.* 4, 044003. <https://doi.org/10.1088/1748-9326/4/4/044003>.
- Sen, P.K., 1968. Estimates of the regression coefficient based on Kendall's Tau. *J. Am. Stat. Assoc.* 63, 1379. <https://doi.org/10.2307/2285891>.
- Seto, K.C., Fragkias, M., Güneralp, B., Reilly, M.K., 2011. A meta-analysis of global urban land expansion. *PLoS One* 6, e23777. <https://doi.org/10.1371/journal.pone.0023777>.
- Small, C., 2001. Estimation of urban vegetation abundance by spectral mixture analysis. *Int. J. Remote Sens.* 22, 1305–1334. <https://doi.org/10.1080/01431160151144369>.
- Small, C., Lu, J.W.T., 2006. Estimation and vicarious validation of urban vegetation abundance by spectral mixture analysis. *Remote Sens. Environ.* 100, 441–456. <https://doi.org/10.1016/J.RSE.2005.10.023>.
- Statistics Canada, 2011. Census Dictionary [WWW Document]. Stat. Canada Cat. no. 98-301-X2011001. Ottawa. URL <https://www12.statcan.gc.ca/census-recensement/2011/ref/dict/geo021-eng.cfm> (Accessed 11.6.18).
- Statistics Canada, 2016. The Changing Landscape of Canadian Metropolitan Areas, Human Activity and the Environment [WWW Document]. Stat. Canada Cat. no. 16-201-X. Ottawa. URL <https://www150.statcan.gc.ca/n1/pub/16-201-x/16-201-x2016000-eng.htm> (accessed 1.9.19).
- Statistics Canada, 2017a. Population Size and Growth in Canada: Key Results From the 2016 Census [WWW Document]. Dly. URL <https://www150.statcan.gc.ca/n1/daily-quotidien/170208/dq170208a-eng.htm> (Accessed 1.9.19).
- Statistics Canada, 2017b. 2016 Census of Canada (Canada, Provinces, Territories, Census Divisions (CDs), Census Subdivisions (CSDs) and Dissemination Areas (DAs)) [WWW Document] (database). URL https://www12.statcan.gc.ca/census-recensement/2016/dp-pd/prof/details/download-telecharger/comp/page_dl-tc.cfm?Lang=E (Accessed 7.24.19).
- Statistics Canada, 2018. Canada goes urban [WWW Document]. Daily, Spec. Interes. Can. Megatrends.
- Theil, H., 1992. A Rank-Invariant Method of Linear and Polynomial Regression Analysis. Springer, Dordrecht, pp. 345–381. https://doi.org/10.1007/978-94-011-2546-8_20.
- Thomas, L.G., 1975. No title. *The Prairie West to 1905: A Canadian Sourcebook*. Oxford University Press, Incorporated.
- Tooke, T.R., Coops, N.C., Goodwin, N.R., Voogt, J.A., 2009. Extracting urban vegetation characteristics using spectral mixture analysis and decision tree classifications. *Remote Sens. Environ.* 113, 398–407. <https://doi.org/10.1016/j.rse.2008.10.005>.
- Tooke, T.R., Klinkenberg, B., Coops, N.C., 2010. A geographical approach to identifying vegetation-related environmental equity in Canadian cities. *Environ. Plan. B Plan. Des.* 37, 1040–1056. <https://doi.org/10.1068/b36044>.
- Turcotte, M., 2008. The city/suburb Contrast: How Can We Measure It? Ottawa, ON. URL <https://doi.org/Catalogueno.11-008-X>.
- Un-Habitat, 2016. Planning Sustainable Cities. Routledge. <https://doi.org/10.4324/9781315541389>.
- United Nations, P.Dofthe Dof Eand S.A., 2018. *World Urbanization Prospects: The 2018 Revision*.
- van den Bosch, M., Bird, W., 2018. Oxford Textbook of Nature and Public Health: the Role of Nature in Improving the Health of a Population - Oxford Medicine. Oxford Univ. PressURL <https://doi.org/10.1093/med/9780198725916.001.0001>.
- van den Bosch, M., Sang, Ode, 2017. Urban natural environments as nature-based solutions for improved public health – a systematic review of reviews. *Environ. Res.* 158, 373–384. <https://doi.org/10.1016/j.envres.2017.05.040>.
- van Leeuwen, W.J.D., Orr, B.J., Marsh, S.E., Herrmann, S.M., 2006. Multi-sensor NDVI data continuity: uncertainties and implications for vegetation monitoring applications. *Remote Sens. Environ.* 100, 67–81. <https://doi.org/10.1016/J.RSE.2005.10.002>.
- Vikhamar, D., Solberg, R., 2003. Snow-cover mapping in forests by constrained linear spectral unmixing of MODIS data. *Remote Sens. Environ.* 88, 309–323. <https://doi.org/10.1016/J.RSE.2003.06.004>.
- Ward, J.H., 1963. Hierarchical grouping to optimize an objective function. *J. Am. Stat. Assoc.* 58, 236–244. <https://doi.org/10.1080/01621459.1963.10500845>.
- White, J.C., Wulder, M.A., Hobart, G.W., Luther, J.E., Hermosilla, T., Griffiths, P., Coops, N.C., Hall, R.J., Hostert, P., Dyk, A., Guindon, L., 2014. Pixel-based image compositing for large-area dense time series applications and science. *Can. J. Remote Sens.* 40, 192–212. <https://doi.org/10.1080/07038992.2014.945827>.
- Wilcox, R.R., 2010. Measuring and detecting associations: methods based on robust regression estimators or smoothers that allow curvature. *Br. J. Math. Stat. Psychol.* 63, 379–393. <https://doi.org/10.1348/000711009X467618>.
- Woodcock, C.E., Allen, R., Anderson, M., Belward, A., Bindschadler, R., Cohen, W., Gao, F., Goward, S.N., Helder, D., Helmer, E., Nemani, R., Oreopoulos, L., Schott, J., Thenkabail, P.S., Vermote, E.F., Vogelmann, J., Wulder, M.A., Wynne, R., 2008. Free access to Landsat imagery. *Science* 320, 1011. <https://doi.org/10.1126/science.320.5879.1011a>.
- Wulder, M.A., Coops, N.C., 2014. Satellites: make earth observations open access. *Nature* 513, 30–31. <https://doi.org/10.1038/513030a>.
- Zhao, S., Zhou, D., Zhu, C., Sun, Y., Wu, W., Liu, S., 2015. Spatial and temporal dimensions of urban expansion in China. *Environ. Sci. Technol.* 49, 9600–9609. <https://doi.org/10.1021/acs.est.5b00065>.
- Zhao, S., Liu, S., Zhou, D., 2016. Prevalent Vegetation Growth Enhancement in Urban Environment 113. pp. 6313–6318. <https://doi.org/10.1073/pnas.1602312113>.
- Zhu, Z., Zhou, Y., Seto, K.C., Stokes, E.C., Deng, C., Pickett, S.T.A., Taubenhöck, H., 2019. Understanding an urbanizing planet: strategic directions for remote sensing. *Remote Sens. Environ.* 228, 164–182. <https://doi.org/10.1016/J.RSE.2019.04.020>.